3-14-2002

Siva-1 binds to and inhibits BCL-XL-mediated protection against UV radiation-induced apoptosis

Li Xue

Fei Chu

Yuan Cheng

Xiangjie Sun

Alip Borthakur
Marshall University, borthakur@marshall.edu

See next page for additional authors

Authors

Li Xue, Fei Chu, Yuan Cheng, Xiangjie Sun, Alip Borthakur, Manjunath Ramarao, Pramod Pandey, Mei Wu, Stuart F. Schlossman, and Kanteti V. S. Prasad

Siva-1 binds to and inhibits BCL-X$_L$-mediated protection against UV radiation-induced apoptosis

Li Xue*†, Fei Chu‡, Yuan Cheng*, Xiangjie Sun‡, Alip Borthakur‡, Manjunath Ramarao†§, Pramod Pandey†¶, Mei Wu∥, Stuart F. Schlossman*†, and Kanteti V. S. Prasad‡**

*Cancer Immunology and AIDS and ¶Adult Oncology, Dana–Farber Cancer Institute, Boston, MA 02115; §Department of Neurology and †Harvard Medical School, Boston, MA 02115; ∥Department of Pathology, Baylor College of Medicine, Houston, TX 77030; and ‡Department of Microbiology and Immunology, University of Illinois at Chicago, Chicago, IL 60612

Contributed by Stuart F. Schlossman, March 28, 2002

We previously cloned Siva-1 by using the cytoplasmic tail of CD27, a member of the tumor necrosis factor receptor family, as the bait in the yeast two-hybrid system. The Siva gene is organized into four exons that code for the predominant full-length Siva-1 transcript, whereas its alternate splice form, Siva-2, lacks exon 2 coding sequence. Various groups have demonstrated a role for Siva-1 in several apoptotic pathways. Interestingly, the proapoptotic properties of Siva-1 are lacking in Siva-2. The fact that Siva-1 is partly localized to mitochondria despite the absence of any mitochondrial targeting signal, it harbors a 20-aa-long putative amphipathic helical structure that is absent in Siva-2, and that its expression is restricted to double-positive (CD3$^+$, CD4$^+$, CD8$^+$) thymocytes like BCL-X$_L$, prompted us to test for a potential interaction between Siva-1 and BCL-X$_L$. Here, we show that Siva-1 binds to and inhibits BCL-X$_L$-mediated protection against UV radiation-induced apoptosis. Indeed, the unique amphipathic helical region (SAH) present in Siva-1 is required for its binding to BCL-X$_L$ and sensitizing cells to UV radiation. Natural complexes of Siva-1/BCL-X$_L$ are detected in HUT78 and murine thymocyte, suggesting a potential role for Siva-1 in regulating T cell homeostasis.

Apoptosis, or programmed cell death, and cell survival are intimately connected, and any shift in the equilibrium between these two important cell functions can cause disease. The principal mediators belong to the BCL-2 and tumor necrosis factor receptor (TNFR) families (1–3). The discovery of BCL-2, a powerful promoter of cell survival, was soon followed by the identification of several proteins with structural similarity to BCL-2. There are four regions of homology termed BH domains; BCL-2 and BCL-X$_L$ have all four domains, whereas BAX and BAK, the proapoptotic members of the family, lack the BH4 domain. Also included in this family are several potent apoptotic molecules that have only a minimal BH3 domain (BAD and BID) (1–3).

BCL-2 and BCL-X$_L$ have a conserved transmembrane region (TM) toward the carboxy terminus that localizes these proteins to the outer mitochondrial membrane, the outer leaflet of the nuclear membrane, and the endoplasmic reticulum. The bulk of the protein projects into the cytoplasm. Although BAX has such a TM region, in normal cells, it appears to be cytosolic and localizes to the mitochondria upon induction of apoptosis. The principal site of action for the BCL-2 family members seems to be the mitochondria (4–6). The proapoptotic members bind via their BH3 domain to the cleft formed by the BH1, BH2, and BH3 domains of the antiapoptotic members BCL-2 and BCL-X$_L$ (1–3, 7). Interestingly, the BH3 domain is a part of the amphipathic helix, underscoring the importance of the amphipathic helical structures in protein–protein interactions.

Various members of the TNFR family regulate cell proliferation and death by means of their interaction with specific intracellular signaling molecules that can be divided broadly into two groups based on the presence of either a death or a TNFR-associated factor (TRAF) domain (1). By using the cytoplasmic tail of CD27, a member of the TNFR family, as the bait in the yeast two-hybrid system, we originally cloned Siva-1 (8, 9), which was subsequently shown to play a role in multiple apoptotic pathways (10–14). The fact that it has a death TRAF domain and, in addition, that its cysteine-rich carboxy terminal region has a zinc finger composed of only cysteines makes Siva-1 unique.

Although Siva-1 lacks any of the known BH domains, we show that it specifically interacts with BCL-X$_L$ through a 20-aa long amphipathic helix, and that it inhibits BCL-X$_L$-mediated protection against UV radiation-induced apoptosis.

Materials and Methods

Reagents. The antibodies used in this study are commercially available [anti-green fluorescent protein (GFP) rabbit antibody, anti-glutathione *S*-transferase (GST) mouse monoclonal, anti-BCL-X$_L$ mouse monoclonal, and anti-BCL-2 mouse monoclonal were obtained from Santa Cruz Biotechnology, the anti-CD3ε mouse was from PharMingen]; the rabbit polyclonal anti-BCL-X$_L$ was the kind gift of L. Boise (Univ. of Miami, Miami, FL). The generation of anti-Siva rabbit antiserum has been described (9). Mitotracker Green FM and Hoechst 33342 were obtained from Molecular Probes. The HeLa cells permanently transfected with pEGFP and pEGFP-BCL-X$_L$ plasmids were the kind gift of W. Marshall (Univ. of Massachusetts, Worcester, MA), and we generated the MCF7 transfectants expressing GFP and GFP-BCL-X$_L$.

Molecular Modeling. The secondary structure predictions are according to Garnier *et al.* (15) and NNPREDICT program. The modeling of the SAH was done as a right-handed α-helix by using INSIGHT II, V.98 (Micron Separations) on a Silicon Graphics Iris workstation.

Various Constructs and Recombinant Proteins. Siva-1 and -2 were cloned inframe into pMT2 vector in the EcoR1 site downstream of GST. The Siva1-Δ36–55 and Δ130–149 deletion mutants were generated by using the QuickChange mutagenesis kit from Stratagene and pMT2-GST-Siva-1 as the template. The fidelity of the constructs was confirmed by sequencing. By using the pGEX system, the GST and GST-Siva-1 proteins were expressed in DH5α and purified according to the manufacturer's protocol (Amersham Pharmacia); the generation of the BCL-X$_L$ fragment (lacking the 20 amino acids from the carboxy terminus) has been described (16).

Protein and Immunoprecipitations. To demonstrate direct binding, varying amounts of recombinant purified BCL-X_L protein were mixed with 25 μg of purified GST or GST-Siva-1 protein, and glutathione Sepharose 4B beads were used to precipitate the GST protein complexes. The binding between Siva-1 and BCL-X_L in Cos-7 cells using transient transfections was demonstrated as described (8, 9), except that we also used sodium deoxycholate (0.1%) in addition to Nonidet P-40 (1% vol/vol) both for lysis and for washing the GST protein precipitates. GFP and the GST proteins were visualized by using anti-GFP rabbit antiserum (1:1,000) and anti-GST monoclonal antibodies (1:500) respectively. Whole-cell lysates (WCLs) were monitored for relative levels of protein expression by immunoblotting. Natural complexes of Siva-1 and BCL-X_L were detected by using anti-BCL-X_L antibody beads and anti-rabbit IgG beads coated with anti-Siva antibody. In competition experiments, varying concentrations of the 20-aa-long synthetic SAH peptide or an equivalent irrelevant peptide were directly added to the cell lysates followed by protein precipitation using glutathione Sepharose 4B beads.

Immunofluorescence Staining, Confocal Microscopy, and Flow Cytometry. HeLa and COS-1 cells were transiently transfected with pSR α-Siva-1-HA with or without the pEGFP-BCL-X_L plasmid. After 2 days, the cells were washed and fixed with paraformaldehyde and permeabilized with 0.1% Triton X-100. Nonspecific binding was blocked with goat serum and then treated with rhodamine-conjugated anti-HA antibody (1:200). To demonstrate colocalization of Siva-1 to mitochondria, we used HeLa cells expressing Siva-1-HA protein and mitotracker Green FM. Distribution of Siva-1 in various types of murine thymocytes isolated from newborn mice thymuses was determined essentially as described (17). After differentially labeling CD4 and CD8, the thymocytes were permeabilized (0.1% Nonidet P-40), blocked with normal goat serum (20% vol/vol), and then treated with anti-Siva rabbit antibody followed by anti-rabbit Ig-FITC (raised in goat). A FACScan cytometer (Becton Dickinson) and CELLQUEST software were used to analyze and represent data.

Apoptosis Assay. MCF7 permanent transfectants were transiently transfected with the various plasmids by using Lipofectamine and a day later were exposed to UV radiation (2 mJ/cm^2 for 1 min). After 5 h, the cells were treated with Hoechst 33342 (1 μg/ml) and incubated at 37°C for 10 min. The cells and their nuclei were photographed with an inverted UV microscope (Nikon Diaphot 200) and analyzed by IMAGE-PRO software. The condensed apoptotic nuclei were physically counted in seven randomly chosen areas.

Results

The human Siva gene is located on the negative strand of human chromosome 14(q32–33) (TPA: BK000018). Similar to mouse, the human gene is organized into four exons coding the full-length predominant form, Siva-1. Its minor alternate splice form, Siva-2, lacks the exon 2 coding region (9). Because of the strong similarity between human and mouse Siva genes, we have numbered the amino acids in human Siva-1 starting with the second ATG as the true start codon. Several reasons led us to investigate the relationship between Siva-1 and BCL-X_L. First, analysis of the region coded by exon 2 in Siva-1 and missing in Siva-2 revealed a highly conserved 20-aa region (Fig. 1*A Top*) that can potentially form an amphipathic helix (SAH; shown as a pinwheel structure in Fig. 1*A Middle*; the space-filling model of the same is depicted in Fig. 1*A Lower*). The region modeled is slightly larger than a BH3 domain of BID and BAD. However, there is no homology at the level of primary sequence between the SAH and BH3 domains. Second, Siva-1 was observed to localize partly to mitochondria. HA-tagged Siva-1 was transiently expressed in HeLa cells, probed with anti-HA-rhodamine
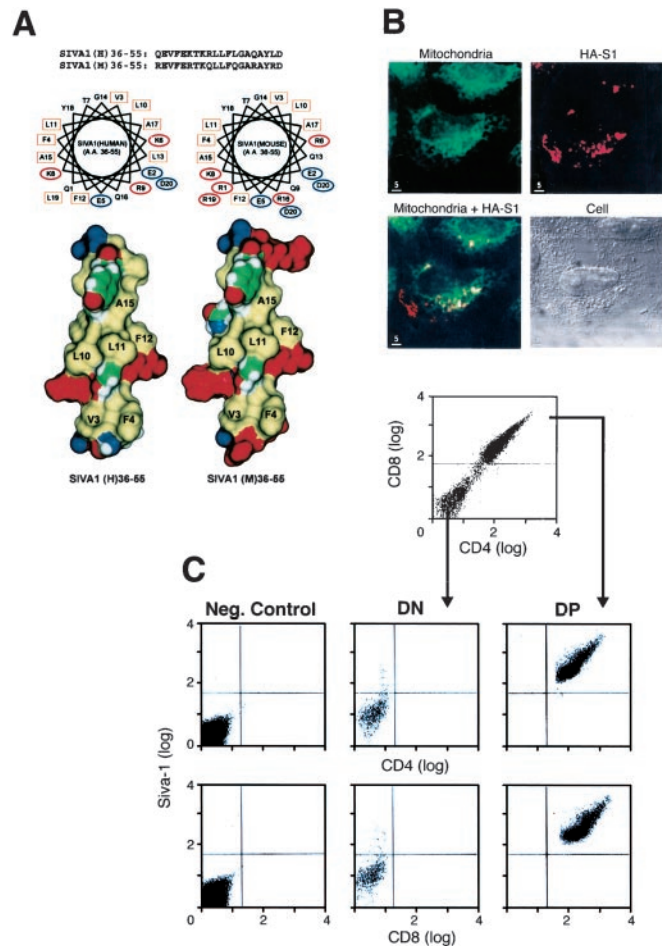

Fig. 1. (*A*) The sequence in Siva-1 corresponding to the predicted amphipathic helix (*Top*), its pinwheel representations (*Middle*), and Connolly space-filling models (*Bottom*) are shown. The hydrophobic face of the helix is shown in the model. The hydrophobic (yellow), the positively charged (red), and the negatively charged (purple) amino acids are shown. The number of the amino acid corresponds to the numbering shown in the pinwheel representation, with one corresponding to 36 and 20 to 55. (*B*) Intracellular distribution of expressed Siva-1-HA in HeLa cells was determined by using anti-HA-rhodamine antibody and Mitotracker Green-FM. Siva-1 is predominantly in the cytoplasm, (*Upper Right*, red), the green specks represent mitochondria in the same cell (*Upper Left*), and the superimposition of the two suggests localization of Siva-1 to mitochondria (*Lower Left*). The morphology of the cell is shown on the lower right. (*C*) Siva-1 is expressed mostly in DP murine thymocytes as evidenced from multicolor flow cytometry (*Right*). The cells treated under similar conditions with isotype control or secondary antibodies failed to label the cells (*Left*).

antibody, and visualized by confocal microscopy. Expression of Siva-1 was mostly in the cytoplasm (Fig. 1*B Upper Right*, red), and the same cell costained with FITC-conjugated-mitochondrial tracker dye revealed mitochondria as green specks (*Upper Left*). Superimposition of the two (*Lower Left*) demonstrated a significant portion of Siva-1 localized to mitochondria (yellow). Empty vector-transfected cells under similar conditions did not reveal any significant fluorescence (data not shown). The cell boundary and its nucleus are pictured in the lower right hand corner. Third, we know that Siva-1 transcripts are highly expressed in human (8) and mouse thymus (data not shown). Analysis of Siva-1 distribution by flow cytometry in newborn mouse thymocytes (Fig. 1*C*), which has mostly double-negative (DN) (CD3$^+$, CD4$^-$, CD8$^-$) and double-positive (DP) thymocytes (CD3$^+$, CD4$^+$, CD8$^+$) revealed that almost all of the DP but not the DN
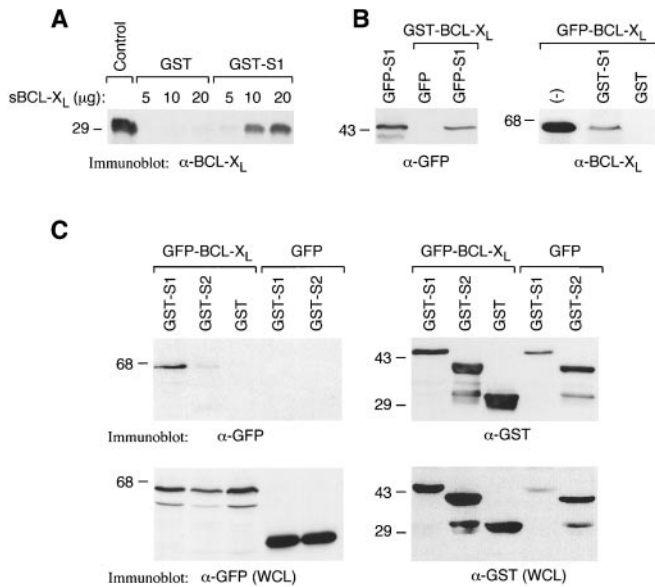
Fig. 2. (A) Direct binding between BCL-X$_L$ and Siva-1. Recombinant GST-Siva-1 and GST when mixed with soluble BCL-X$_L$ resulted in a dose-dependent direct interaction between GST-Siva-1 and BCL-X$_L$, despite GST being far in excess of GST-Siva-1. (B) Recombinant purified GST-Siva-1 and GST-BCL-X$_L$ proteins individually could be used to coprecipitate GFP-BCL-X$_L$ and GFP-Siva-1, respectively, from cell lysates. Cos cells were transiently transfected with pEGFP-Siva-1 or pEGFP-BCL-X$_L$, lysed, and mixed with equivalent amounts of either GST-Siva-1 or GST-BCL-XL proteins. The GST protein complexes were precipitated as described in *Methods* and immunoblotted with anti-GFP and anti-BCL-XL antibodies. The first lanes (both *Left* and *Right*) represent the relative amounts of the GFP proteins expressed in the WCLs. (C) GST-Siva-1 but not GST or GST-Siva-2 binds to GFP-BCL-X$_L$. Cos cells were transiently transfected with GFP-BCL-X$_L$ and GST- or GST-Siva-1- or GST-Siva-2-expressing plasmids. After 48 h, the cells were lysed, and the GST protein complexes were collected and subjected to SDS/PAGE followed by immunoblotting with anti-GFP antibody. As shown in the top left hand corner, a significant amount of GFP-BCL-X$_L$ was seen only in the lane corresponding to GST-Siva-1. GFP itself did not bind to either GST-Siva-1 or GST-Siva-2, as shown by cotransfection of the empty GFP plasmid with GST-Siva-1 or GST-Siva-2. The same blot was stripped and probed with ant-GST antibody to demonstrate that various GST proteins are indeed precipitated (*Top Right*). The relative levels of expressed GFP and GST proteins in the WCLs are also shown (*Bottom*, *Left* and *Right*, respectively).

thymocytes expressed Siva-1, a pattern mirroring BCL-X$_L$ expression (18). Similarly tagged secondary antibodies or normal serum isotype antibodies failed to label the cells significantly under comparable conditions. We next investigated the possibility that Siva-1 could interact with BCL-X$_L$.

To demonstrate direct binding between Siva-1 and BCL-X$_L$, we mixed purified bacterial recombinant GST and GST-Siva-1 proteins with increasing amounts of purified BCL-X$_L$ fragment. GST proteins were precipitated from the mixture by using glutathione Sepharose beads, subjected to SDS/PAGE analysis, and then immunoblotted with anti-BCL-X$_L$ antibody (Fig. 2A). GST-Siva-1 but not GST alone coprecipitated BCL-X$_L$ with increasing amounts of soluble BCL-X$_L$, demonstrating direct interaction between Siva-1 and BCL-X$_L$. Also, GST-Siva-1 and GST-BCL-X$_L$ proteins were used to pull down GFP-BCL-X$_L$ and GFP-Siva-1, respectively, from 293T cell lysates (Fig. 2B). Recombinant GST-BCL-X$_L$ precipitated transiently expressed GFP-Siva-1 but not GFP (Fig. 2B *Left*), and GST-Siva-1 but not GST selectively brought down GFP-BCL-X$_L$ (*Right*). WCLs were assessed for relative levels of GFP-Siva-1 and GFP-BCL-X$_L$ expression; they were comparable (data not shown). Cotransfection of COS-1 cells with GFP-BCL-X$_L$ and GST- or GST-

Siva-1- or GST-Siva-2-expressing plasmids, demonstrated the specific interaction between BCL-X$_L$ and Siva-1. Immunoblotting with anti-GFP antibodies revealed that GST-Siva-1 but not GST-Siva-2 or GST is able to coprecipitate GFP-BCL-X$_L$ from the double transfectants, and GFP is unable to associate with any of the GST fusion proteins (Fig. 2C; upper left-hand corner, compare lane 1 with 2 and 3). The same blot was stripped and probed with anti-GST antibody to demonstrate that the relevant GST proteins were precipitated from the WCLs (upper right-hand corner). The relative levels of the expressed proteins in the WCLs can be seen in the lower panel. Although expression of GST-Siva-1 is low in comparison to GST-Siva-2 or GST, only GST-Siva-1 could coprecipitate a significant amount of BCL-X$_L$.

To rule out potential artifacts generated because of cell lysis, the intracellular colocalization of Siva-1 and BCL-X$_L$ was verified. We transiently coexpressed GFP-BCL-X$_L$ and Siva-1-HA in HeLa cells and detected their localization by using anti-HA-rhodamine antibodies, which were visualized by confocal microscopy (Fig. 3A). The pattern of cellular expression of BCL-X$_L$ (green) and Siva-1 (red) shown in (*Left*) and (*Middle*), respectively, are very similar. The two patterns are highly superimposable (yellow) with punctate distribution around the nucleus characteristic of mitochondrial expression, favoring Siva-1/BCL-X$_L$ interaction in the cell. By using detergent lysates of murine thymocytes isolated from newborn mice thymuses, we immunoprecipitated BCL-X$_L$ complexes by using anti-BCL-X$_L$ antibody beads (Fig. 3B). Anti-mouse IgG beads served as a negative control. Relatively low amounts of Siva-1 were coprecipitated with BCL-X$_L$. However, the amount of Siva-1 increased dramatically after CD3 receptor crosslinking for 30′, but after 1 and 2 h, it drastically decreased, accompanied by a shift in its mobility. In parallel immunoblotting experiments, we verified that the anti-BCL-X$_L$ beads used did precipitate BCL-X$_L$, and that the protein band seen at about 20 kDa in anti-BCL-X$_L$ immunoprecipitates was similar to the band seen in anti-Siva immunoprecipitates (data not shown). With untreated HUT78 cells (Fig. 3C), we observed that a significant amount of Siva-1 coprecipitated with BCL-X$_L$ but not with BCL-2 or with the secondary antibody-conjugated beads (*Upper*). Additionally, we detected a significant presence of BCL-X$_L$ in anti-Siva immunoprecipitates but not in other control immunoprecipitations (*Lower*). Exposure to UV radiation followed by incubation for 30 min resulted in a slight increase in the amount of the Siva-1/BCL-X$_L$ complex (*Upper*). Although we could detect BCL-X$_L$ in anti-Siva immunoprecipitate at 60 min, we could not detect any coprecipitated Siva-1 with BCL-X$_L$ (compare *Upper* and *Lower*). This anomaly could be because of different affinities and avidities of the two antibodies used. The fact that the anti-BCL-2 antibody used did precipitate BCL-2 was confirmed in other experiments (data not shown).

Next, we determined the BCL-X$_L$ interacting site in Siva-1. Data obtained from several deletion and point mutants suggested that the SAH region in Siva-1 could indeed be the principal mediator of binding to BCL-X$_L$ (Fig. 4). To obtain unambiguous results, we expressed GST-Siva-1ΔSAH and an equivalent control mutant (Siva-1-Δ130–149) in conjunction with GFP-BCL-X$_L$ in Cos cells (Fig. 4A) and screened for binding. Protein precipitations revealed significant amounts of GFP-BCL-X$_L$ in the lanes corresponding to either GST-Siva-1 or GST-Siva-1Δ130–149 but not GST-Siva-1ΔSAH, demonstrating that the SAH region in Siva-1 is essential for binding to BCL-X$_L$. Relative levels of GST fusion proteins (*Middle*) and GFP-BCL-X$_L$ (*Lower*) in the WCLs were comparable.

The ability of the SAH and an unrelated peptide to displace GFP-BCL-X$_L$ bound to GST-Siva-1 was then determined. Cell lysates prepared from Cos-1 cells transiently transfected with GST-Siva-1 and GFP-BCL-X$_L$ encoding plasmids were challenged with varying concentrations of the SAH or a control
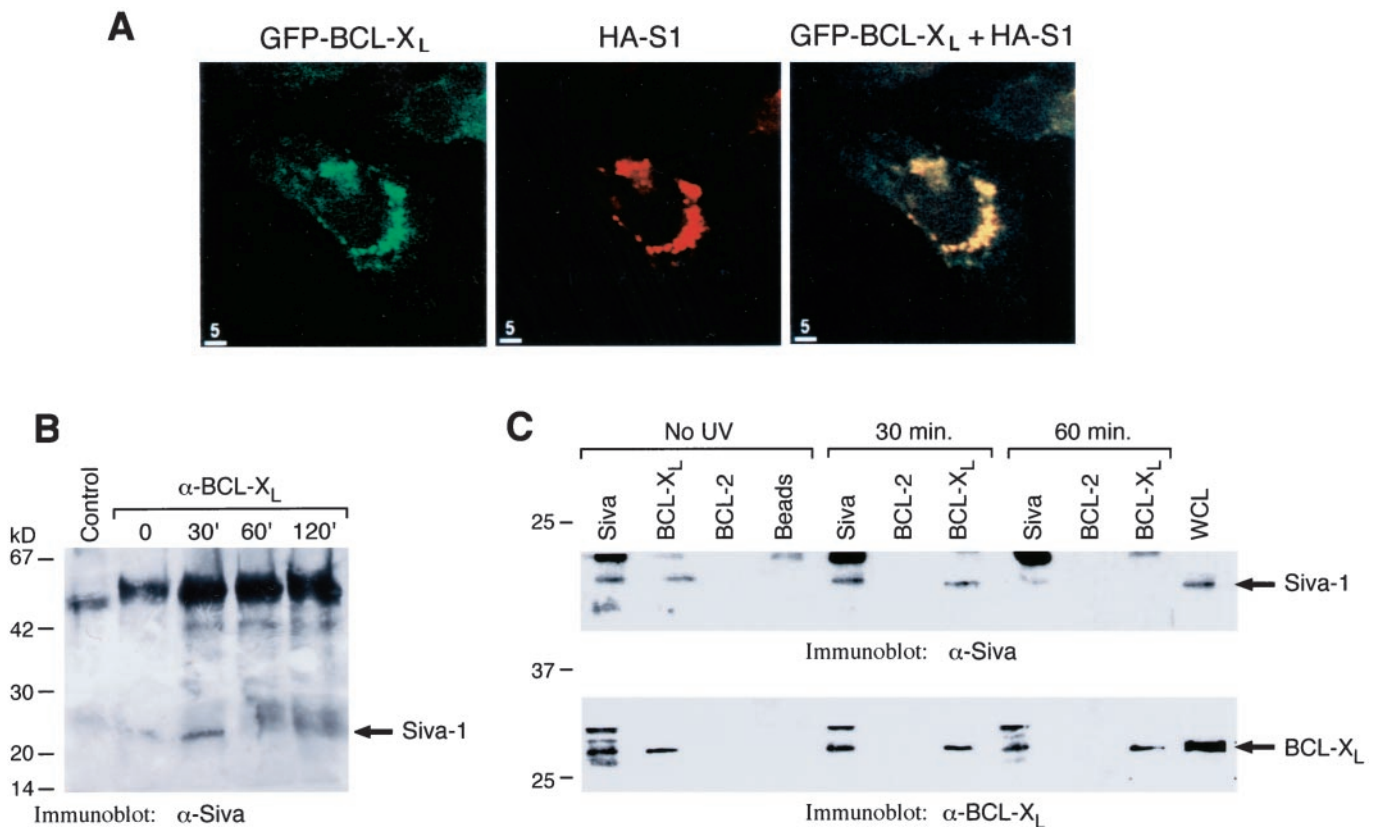
Fig. 3. (A) HA-tagged Siva-1 and GFP-BCL-X$_L$ were expressed together in HeLa cells and stained with anti-HA-rhodamine antibody. Most of the expressed Siva-1 (red) and BCL-X$_L$ (green) colocalize to the same intracellular compartment as seen in the superimposed picture (yellow). (B) The kinetics of natural Siva-1/BCL-X$_L$ complexes in murine thymocytes after CD3 crosslinking is shown. Thymocytes obtained from thymuses of newborn mice were cultured on plates coated with anti-mouse CD3 antibody for the indicated times. Cells (100×10^6 per sample) were lysed and immunoprecipitated with either anti-rabbit Ig beads (control) or anti-BCL-X$_L$ antibody-linked beads and subjected to immunoblotting with anti-Siva rabbit polyclonal antibody. The amount of coprecipitated Siva-1 increased by 30′ and then decreased, and in the control lane, it did not reveal the presence of significant amount of Siva-1. Immunoblotting with the secondary antibody alone did not reveal any bands in the corresponding region shown in the figure (data not shown). (C) Hut78 cells were exposed to UV and then incubated for 30 and 60 min, lysed, and subjected to immunoprecipitations. (*Upper*) Immunoblot probed with anti-Siva antibody. The same blot was stripped and probed with anti-BCL-X$_L$ antibody (*Lower*). The vertical labels represent various immunoprecipitations. In Hut78 cells not exposed to UV radiation, a significant amount of Siva-1 was found to be associated with BCL-X$_L$ (lane 2, *Upper*), and the reverse can be seen in the lower panel (lane 1), wherein BCL-X$_L$ is coprecipitated with Siva-1 in anti-Siva immunoprecipitates. Secondary antibody-conjugated beads alone or anti-BCL-2 antibody immunoprecipitates did not bring down Siva-1 or BCL-X$_L$. The amount of Siva-1 in BCL-X$_L$ immunoprecipitate increased slightly by 30 min after exposure to UV radiation, and then decreased by 60 min to undetectable levels (*Upper*); however, at this time point, BCL-X$_L$ could still be found in Siva-1 immunoprecipitate (*Lower*). The expression of endogenous Siva-1 and BCL-XL in the WCLs is also shown (last lanes, *Upper* and *Lower*).

irrelevant peptide; the GST protein precipitates then were analyzed for the presence of coprecipitated GFP-BCL-X$_L$. GST-Siva-1 but not GST coprecipitated a significant amount of GFP-BCL-X$_L$ (Fig. 4B, lane 1) and even at the maximum concentration of the control peptide tested (200 μM), a significant amount of GFP-BCL-X$_L$ coprecipitated with GST-Siva-1 (lane 5). However, by using increasing concentrations of the SAH peptide, we could compete off the GST-Siva-1-bound GFP-BCL-X$_L$ with complete inhibition of binding at 100 μM of peptide (lane 2). Relative levels of the GFP and GST fusion proteins in the WCLs were comparable (Fig. 4C).

To analyze the functional significance of the Siva-1–BCL-X$_L$ interaction, we used polyclonal stable MCF7 cells that express GFP or GFP-BCL-X$_L$. As expected, GFP-BCL-X$_L$ transfectants were highly resistant to UV-induced apoptosis (19), compared with GFP transfectants (Fig. 5A); only transfection of GST-Siva-1 but not GST-Siva-2 or GST resulted in abrogation of BCL-X$_L$-mediated protection (Fig. 5B). Representative pictures of condensed apoptotic nuclei as evidenced by Hoechst staining are shown in Fig. 5C. The data obtained by using various deletion mutants of Siva-1 confirmed our suspicion that the SAH region

in Siva-1 is required for binding to BCL-X$_L$ and inhibition of BCL-X$_L$ function (Fig. 5). The deletion of the SAH domain in Siva-1 resulted in a complete loss of the mutant's ability to suppress BCL-X$_L$ function, whereas an equivalent deletion toward the carboxy terminus had no effect (Fig. 5D). Relative levels of expressed proteins were monitored separately and found to be comparable (data not shown).

Discussion

Siva-1 is a relatively small proapoptotic molecule we initially discovered by using the cytoplasmic tail of CD27 (a member of the TNFR family) as the bait in a yeast two-hybrid system (8). Unlike Fas and TNFR1, CD27 lacks a death domain in its relatively short cytoplasmic tail and yet can induce apoptosis. Several members of the TNFR family that lack a death domain can also induce apoptosis (20, 21). Siva-1, by interacting with CD27, probably facilitates cell death by an as-yet-unknown mechanism. However, several published papers from our group and others (22–24) and a study using CD27 knockouts (25) supports a role for CD27 in costimulation. This finding is not surprising, given the fact that the apoptotic pathways are redun-
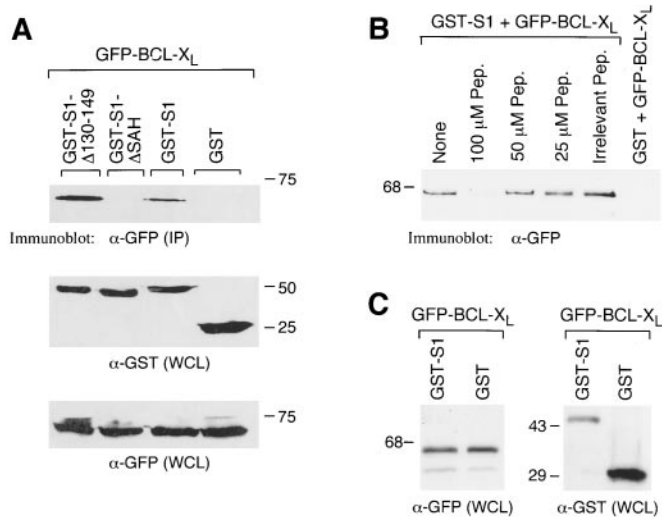
Fig. 4. (*A*) Deletion of the SAH region in Siva-1 but not an unrelated downstream region results in loss of BCL-X$_L$ binding. Various plasmids were coexpressed with pEGFP-BCL-X$_L$ in Cos cells and the lysates were subjected to protein precipitations by using the glutathione beads. α-GFP immunoblot (*Top*) demonstrates coprecipitation of GFP-BCL-X$_L$ with the control deletion (GST-Siva-1Δ130–149) but not SAH deletion mutant of Siva-1 (GST-Siva-1Δ36–55). Relative levels of GST-fusion proteins in the WCLs (*Middle*). Expression of GFP-BCL-X$_L$ (*Bottom*). (*B*) SAH peptide but not excess of irrelevant peptide competes off GFP-BCL-X$_L$ bound to GST-Siva-1. To the lysates containing expressed GST-Siva-1 and GFP-BCL-X$_L$, various concentrations of the SAH peptide or irrelevant peptide (200 μM) were added, and the GST-Siva-1 protein complexes were immunoblotted with anti-GFP antibody. The GFP-BCL-X$_L$ bound to GST-Siva-1 (lane 1) was competed off completely at 100 μM SAH peptide (lane 2) but not with irrelevant peptide at 200 μM (lane 5). GST alone did not coprecipitate any GFP-BCL-X$_L$ (lane 6). (*C*) The left-hand panel represents the relative expression of GFP-BCL-X$_L$; the right-hand panel represents the relative expression of the GST and GST-Siva-1 proteins in the WCLs used in the competition experiment shown in *B*.

Fig. 5. (*A*) GFP but not GFP-BCL-X$_L$ stable MCF7 transfectants are highly susceptible to UV radiation-induced apoptosis. (*B*) Transient expression of GST-Siva-1 but not GST or GST-Siva-2 results in loss of protection against UV radiation-induced apoptosis in BCL-X$_L$ transfectants. (*C*) Representative pictures of apoptotic nuclei seen in *B* by staining with Hoechst are shown. (*D*) Deletion of the SAH domain in Siva-1 (Δ36–55) but not an irrelevant region (Δ130–149) results in the complete loss of its ability to suppress BCL-X$_L$ function.

dant, and silencing a single gene may not reveal its complete plethora of actions. For instance, lpr mice (Fas knockouts) suffer from lymphoproliferative disorders (26), whereas the TNFR1 knockouts do not exhibit any of the disease symptoms (27), although both are known potent inducers of apoptosis. The Fas/TNFR1 double knockouts however develop with a much more severe form of the disease with an early onset and significantly higher mortality rates than the single Fas knockout mice (28). Thus, it is possible that CD27 may be functioning *in vivo* with other receptors. The antiapoptotic BCL-2 family members do inhibit TNFR1-induced apoptosis (19); however, the physiological relevance of CD27-induced apoptosis and its connection, if any, to Siva-1 and BCL-X$_L$ remains to be established.

The human Siva gene is located on chromosome 14 (q32–33, negative strand) and interestingly, this region is targeted for chromosomal translocation t(14:18)(q32:q21) seen in various lymphomas (reviewed in ref. 3). The regulation of Siva-1 in these cancers remains to be determined. BCL-2 prolongs cell survival and, in cooperation with c-*myc*, can immortalize pre-B cells (29). Overexpression of BCL-2 in B cells and T cells increases the incidence of B cell lymphomas (18) and T cell leukemias (30) and is further enhanced in transgenic mice that also express myc (31). Loss of function mutations in BAX have been linked to increased incidence of cancer (32, 33), thus characterizing BAX as a tumor suppressor. Siva-1 binds to BCL-X$_L$ and abrogates its function, suggesting a possible tumor-suppressor role. A recent study demonstrating the down regulation of Siva gene transcription along with the tumor suppressor p53 and TOSO in colorectal
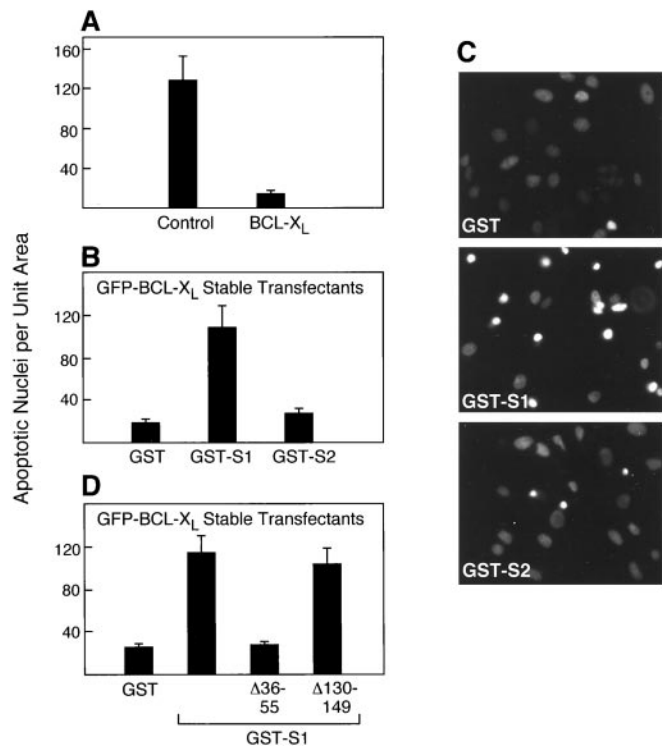
cancer (34) supports this contention. CC2/TIP-30, a Ser-Thr kinase and known metastasis suppressor, when expressed in SCLC (small cell lung cancer) cells, resulted in a substantial increase in the expression of two proapoptotic genes, BAD and Siva, culminating in cell death (12). These studies suggest a potential role for Siva in physiological cell death.

The Siva-1 SAH domain is highly conserved, with 75% identity between human and mouse and 95% identity between mouse and rat (8–10), and seems to be the principal mediator of binding to BCL-X$_L$. The results presented here suggest the possibility of direct binding between Siva-1 and BCL-X$_L$. In experiments demonstrating the interaction between Siva-1 and BCL-X$_L$, we used sodium deoxycholate, an ionic detergent, both for cell lysis and subsequent washes of GST precipitates, suggesting that the interaction between Siva-1 and BCL-X$_L$ is relatively strong. The SAH region has no homology to other known BH3 domains, and, therefore, we anticipate its binding region in BCL-X$_L$ to be unique. This is also supported by the fact that deletion of the first half of the SAH region in Siva-1 results in complete loss of binding to BCL-X$_L$ and inhibition of its function (data not shown). One of the reasons we chose to investigate Siva-1 association with BCL-X$_L$ is that the expression of Siva-1 in thymocytes is similar to that of BCL-X$_L$ (35). *In vivo* studies have clearly demonstrated a role for BCL-X$_L$ in the survival of DP thymocytes (35), and the fact that thymocytes harbor natural complexes of Siva-1/BCL-X$_L$ suggests a physiological antagonistic role for Siva-1 in the survival of DP thymocytes.

CD3 crosslinking and UV radiation induced significant kinetic changes in the Siva-1/BCL-X$_L$ complexes, suggesting a role for other players or posttranslational modifications, as is the case

with some of the BCL-2 family members. For instance, conversion of BID to tBID by active caspase 8 makes its BH3 domain accessible (36, 37). BAD, upon Ser/Thr phosphorylation, is sequestered by 14–3-3 and inactivated (38, 39). We recently showed that Siva-1 binds to ARG (abl-related tyrosine kinase) and is phosphorylated on Y34, rendering cells highly susceptible to reactive oxygen species-induced apoptosis (11). Therefore, it is possible that the observed kinetic changes in Siva-1/BCL-X$_L$

complexes could be the result of posttranslational modifications. Although Siva-1 can bind to and inhibit BCL-X$_L$ function, the *in vivo* functional link between the two remains to be established.

1. Strasser, A., O'Connor, L. & Dixit, V. M. (2000) *Annu. Rev. Biochem.* **69,** 217–245.
2. Adams, J. M. & Cory, S. (2001) *Trends Biochem. Sci.* **26,** 61–66.
3. Korsmeyer, S. J. (1999) *Cancer Res.* **59,** 1693S–1700S.
4. Reed, J. C. & Green, D. R. (2002) *Mol. Cell.* **9,** 1–3.
5. Gross, A., McDonnell, J. M. & Korsmeyer, S. J. (1999) *Genes Dev.* **13,** 1899–1911.
6. Vander Heiden, M. G. & Thompson, C. B. (1999) *Nat. Cell Biol.* **1,** E209–E216.
7. Sattler, M., Liang, H., Nettesheim, D., Meadows, R. P., Harlan, J. E., Eberstadt, M., Yoon, H. S., Shuker, S. B., Chang, B. S., Minn, A. J., Thompson, C. B. & Fesik, S. W. (1997) *Science* **275,** 983–986.
8. Prasad, K. V. S., Ao, Z., Yoon, Y., Wu, M. X., Rizk, M., Jacquot, S. & Schlossman, S. F. (1997) *Proc. Natl. Acad. Sci. USA* **94,** 6346–6351.
9. Yoon, Y., Ao, Z., Cheng, Y., Schlossman, S. F. & Prasad, K. V. (1999) *Oncogene* **18,** 7174–7179.
10. Padanilam, B. J., Lewington, A. J. & Hammerman, M. R. (1998) *Kidney Int.* **54,** 1967–1975.
11. Cao, C., Ren, X., Kharbanda, S., Koleske, A., Prasad, K. V. & Kufe, D. (2001) *J. Biol. Chem.* **276,** 11465–11468.
12. Xiao, H., Palhan, V., Yang, Y. & Roeder, R. G. (2000) *EMBO J.* **19,** 956–963.
13. Henke, A., Launhardt, H., Klement, K., Stelzner, A., Zell, R. & Munder, T. (2000) *J. Virol.* **74,** 4284–4290.
14. Henke, A., Nestler, M., Strunz, S., Saluz, H. P., Hortschansky, P., Menzel, B., Martin, U., Zell, R., Stelzner, A. & Munder, T. (2001) *Virology* **289,** 15–22.
15. Garnier, J., Gibrat, J. F. & Robson, B. (1996) *Methods Enzymol.* **266,** 540–553.
16. Kharbanda, S., Pandey, P., Schofield, L., Israels, S., Roncinske, R., Yoshida, K., Bharti, A., Yuan, Z. M., Saxena, S., Weichselbaum, R., Nalin, C. & Kufe, D. (1997) *Proc. Natl. Acad. Sci. USA* **94,** 6939–6942.
17. Zhang, Y., Schlossman, S. F., Edwards, R. A., Ou, C. N., Gu, J., Wu, M. X. (2002) *Proc. Natl. Acad. Sci. USA* **99,** 878–883.
18. McDonnell, T. J., Deane, N., Platt, F. M., Nunez, G., Jaeger, U., McKearn, J. P. & Korsmeyer, S. J. (1989) *Cell* **57,** 79–88.
19. Srinivasan, A., Li, F., Wong, A., Kodandapani, L., Smidt, R., Jr., Krebs, J. F., Fritz, L. C., Wu, J. C. & Tomaselli, K. J. (1998) *J. Biol. Chem.* **273,** 4523–4529.
20. Amakawa, R., Hakem, A., Kundig, T. M., Matsuyama, T., Simard, J. J., Timms, E., Wakeham, A., Mittruecker, H. W., Griesser, H., Takimoto, H., *et al.* (1996) *Cell* **84,** 551–562.

21. Majdan, M., Lachance, C., Gloster, A., Aloyz, R., Zeindler, C., Bamji, S., Bhakar, A., Belliveau, D., Fawcett, J., Miller, F. D. & Barker, P. A. (1997) *J. Neurosci.* **17,** 6988–6998.
22. Kobata, T., Agematsu, K., Kameoka, J., Schlossman, S. F. & Morimoto, C. (1994) *J. Immunol.* **153,** 5422–5432.
23. Kobata, T., Jacquot, S., Kozlowski, S., Agematsu, K., Schlossman, S. F. & Morimoto, C. (1995) *Proc. Natl. Acad. Sci. USA* **92,** 11249–11253.
24. Gravestein, L. A., Nieland, J. D., Kruisbeek, A. M. & Borst, J. (1995) *Int. Immunol.* **7,** 551–557.
25. Hendriks, J., Gravestein, L. A., Tesselaar, K., van Lier, R. A., Schumacher, T. N. & Borst, J. (2000) *Nat. Immunol.* l433–40.
26. Cohen, P. L. & Eisenberg, R. A. (1993) *Immunol. Today* **13,** 427–428.
27. Pfeffer, K., Matsuyama, T., Kundig, T. M., Wakeham, A., Kishihara, K., Shahinian, A., Wiegmann, K., Ohashi, P. S., Kronke, M. & Mak, T. W. (1993) *Cell* **73,** 457–467.
28. Zhou, T., Edwards, C. K., 3rd, Yang, P., Wang, Z., Bluethmann, H. & Mountz, J. D. (1996) *J. Immunol.* **156,** 2661–2665.
29. Vaux, D. L., Cory, S. & Adams, J. M. (1988) *Nature (London)* **335,** 440–442.
30. Linette, G. P., Hess, J. L., Sentman, C. L. & Korsmeyer, S. J. (1995) *Blood* **86,** 1255–1260.
31. Marin, M. C., Hsu, B., Stephens, L. C., Brisbay, S. & McDonnell, T. J. (1995) *Exp. Cell Res.* **217,** 240–247.
32. Rampino, N., Yamamoto, H., Ionov, Y., Li, Y., Sawai, H., Reed, J. C. & Perucho, M. (1997) *Science* **275,** 967–969.
33. Yin, C., Knudson, C. M., Korsmeyer, S. J. & Van, Dyke, T. (1997) *Nature (London)* **385,** 637–640.
34. Okuno, K., Yasutomi, M., Nishimura, N., Arakawa, T., Shiomi, M., Hida, J., Ueda, K. & Minami, K. (2001) *Dis. Colon Rectum* **44,** 295–299.
35. Ma, A., Pena, J. C., Chang, B., Margosian, E., Davidson, L., Alt, F. W. & Thompson, C. B. (1995) *Proc. Natl. Acad. Sci. USA* **92,** 4763–4767.
36. Li, H., Zhu, H., Xu, C. J. & Yuan, J. (1998) *Cell* **94,** 491–501.
37. Luo, X., Budihardjo, I., Zou, H., Slaughter, C. & Wang, X. (1998) *Cell* **94,** 481–490.
38. Zha, J., Harada, H., Yang, E., Jockel, J. & Korsmeyer, S. J. (1996) *Cell* **87,** 619–628.
39. Wang, H.-G., Pathan, N., Ethell, I. M., Krajewski, S., Yamaguchi, Y., Shibasaki, F., McKeon, F., Bobo, T., Franke, T. F. & Reed, J. C. (1999) *Science* **284,** 339–343.